Available online at www.sciencedirect.com

ScienceDirect

Ceramics International 40 (2014) 13929–13936

CERAMICS INTERNATIONAL

www.elsevier.com/locate/ceramint

Ceramic substrates of β-SiC/SiAlON composite from preceramic polymers and Al–Si fillers

R.M. Rocha[a,*], J.C. Bressiani[b], A.H.A. Bressiani[b]

[a]*Instituto de Aeronáutica e Espaço (IAE), Pça Marechal do Ar Eduardo Gomes 50, Vl. das Acácias, CEP: 12228-904 São José dos Campos, Brazil*
[b]*Instituto de Pesquisas Energéticas e Nucleares (IPEN), Av. Lineu Prestes 2242, Cidade Universitária, CEP: 05508-000 São Paulo, Brazil*

Received 2 April 2014; received in revised form 23 May 2014; accepted 24 May 2014
Available online 2 June 2014

Abstract

Commercial polysilsesquioxanes filled with silicon and aluminum particles were prepared in the form of a thin sheet by tape casting and pyrolyzed in nitrogen atmosphere at various temperatures up to 1500 °C. Two silicone resins with different carbon content were used to prepare slurries containing 30 vol% of Si and Al as filler with volume ratios of 1:1 and 1:3. The crystalline phases that formed in the polymer derived ceramic (PDC) substrates pyrolyzed at different temperatures were identified using x-ray diffraction patterns. Substrates pyrolyzed at 1500 °C were characterized with respect to their density, total open porosity and thermal expansion coefficient. The resulting microstructures were examined using scanning and transmission electron microscopy. The main crystalline phases in substrates pyrolyzed at 1000 °C were identified as Si, β-SiC and AlN. These gradually converted to β-SiC/SiAlON composites at 1500 °C. The higher carbon content favored formation of the phases β-SiC and AlN. The β-SiAlON phase predominated in substrates with higher Si content while SiALON polytypoids were more significant in substrates with higher Al content. The 21R ($SiAl_6O_2N_6$), 12H ($SiAl_5O_2N_5$) and 15R ($SiAl_4O_2N_4$) SiAlON polytypoids were observed in all the samples and were identified by high resolution electron microscopy (HREM) in samples pyrolyzed at 1500 °C.

Keywords: A. Tape casting; Polymer derived ceramic; D. SiC; E.; SiAlON-polytypoid; β-SiAlON

1. Introduction

Polymer derived ceramics (PDCs) offer unique opportunities for making quality ceramic components using plastic technologies, with low processing cost and relatively low processing temperature. However, the applicability of polymer pyrolysis to the fabrication of monolithic components is quite difficult, due mainly to the high volume shrinkage associated with the polymer–ceramic transition that often leads to the development of intrinsic micro-cracks [1]. The introduction of inert and/or active filler powders in the polymer precursor has been used to overcome this problem as it offers the possibility of reducing shrinkage and porosity [2]. Inert powders, such as SiC, will not react with anything during pyrolysis. They simply occupy space to reduce the effective volume of the voids and increase the overall density of the pyrolyzed product. Active fillers powders, however will react with the decomposition products of the polymer or a reactive gas during pyrolysis and will expand to compensate shrinkage of the polymer. In this manner, a near-net-shape conversion can be achieved [3].

One of the advantages of the PDCs is the possibility to use a large variety of different forming methods. Tape casting is an example. Alternative tape casting processing makes use of the rheological properties of viscous preceramic polymer systems. The preceramic polymer acts as a binder at casting temperature and provides ceramic components during thermal conversion. In the presence of ceramic/metallic fillers or in a reactive atmosphere the ceramic residue from preceramic polymer decomposition can react to form new phases. The use of a slurry consisting of polysiloxane preceramic polymer, silane monomers for viscosity control and mixtures of Si–SiC [4] and Si–Al_2O_3 [5] as particulate fillers was already successfully demonstrated for the manufacture of PDC substrates. The proposal of this study was the manufacture of PDC

*Corresponding author. Tel.: +55 12 3947 6441; fax: +55 12 3947 6405.
E-mail address: rosa.rocha11@gmail.com (R.M. Rocha).

http://dx.doi.org/10.1016/j.ceramint.2014.05.114
0272-8842/

substrates in the Si–Al–O–N–C system using a mixture of Al and Si filler powder loaded silane/polysilsesquioxane slurries processed by doctor blade and pyrolyzed in nitrogen atmosphere. Individually, Al and Si powders were the object of many studies as fillers in polymer precursors, but very seldom has the use of both these powders together been studied [6]. For example, loading $CH_3SiO_{1.5}$ with Si powder pyrolyzed in nitrogen atmosphere has proved to be a promising method for in situ formation of Si_2ON_2 at low processing temperatures [7,8]. The influence of Al filler on the pyrolysis of polysiloxanes was investigated intensively, mainly in oxidizing conditions by pyrolysis in air with the goal to obtain SiC- mullite composites [9–11]. Therefore, this work has as its objective to apply Si and Al together as active fillers in polysilsesquioxane to produce a composite ceramic with SiC and phases in the SiAlON system.

Sialons are silicon aluminum oxynitride ceramic materials with a range of technically important applications, since they can have a wide range of compositions and occur in several different families of crystal structures [12]. However, the application of SiAlON ceramics has always been limited by the high cost attributed to the use of high-purity raw materials. Since the end of the 1970s, many investigations were devoted to synthesizing SiAlON using carbothermal reduction and nitridation of low cost raw materials, including clay minerals and industrial wastes [13–16]. More recently, SiAlON-based materials were obtained by PDCs using only alumina nanopowders as filler [17] and mixtures of secondary additives (AlN and Si_3N_4) in silicone resins [18]. Compared to these recent studies, our aim is the application of lower cost materials as filler (Al and Si) in silicone resins to obtain SiAlON phases at low temperatures.

2. Experimental procedure

2.1. Materials

Two types of commercially available polysilsesquioxanes with different physical and chemical properties were chosen as preceramic precursors. A methyl-containing polysilsesquioxane-PMS (MK, general formula of $(CH_3SiO_{1.5})_n$ with $n=130$–150 and melting point of 42 °C) is a powder at room temperature. The second polymer system is a phenyl-containing polysilsesquioxane-PPS (H62C, general formula $[(C_6H_5)_{0.44}(CH_3)_{0.24}(C_2H_3)_{0.16}SiO_{1.5}]_n$), a low viscosity liquid at room temperature. Both precursors are from Wacker AG, Burghausen, Germany. The PMS contains a few mole percent of reactive ethoxy ($-OC_2H_5$) and hydroxyl groups ($-OH$) which undergo a polycondensation reaction upon heating above 150 °C, resulting in the release of water and ethanol. The curing reaction of PPS is also thermally induced and governed by a hydrosilation reaction (β-addition), thanks to the presence of vinyl functional groups at similar temperatures, thus no volatile condensation products are released. The precursors differ in their carbon content, which is 14.8 wt% for PMS [19] and 45.5 wt% for PPS [20]. Methyltrietoxysilane (MTES-$CH_3Si(OC_3H_5)_3$, (Wacker AG, Burghausen, Germany) was used to dissolve the polymers and as a viscosity modifier. Two different catalysts were used for the different cross-linking ranges, oleic acid ($C_{18}H_{34}O_2$) to cross-link the viscosity modifying monomers at room temperature and zirconium acetylacetonate ($C_{20}H_{28}O_8Zr$) for cross-linking of the preceramic polymers at elevated temperatures (~200 °C). Silicon powder (Si, with an average particle size of $d_{50}=3.1$ μm) and Aluminum powder (Al, with an average particle size of $d_{50}=30.0$ μm) were added as reactive fillers.

2.2. Slurry preparation

The volume ratio of filler:polymer precursor was 1:1.5. To obtain optimal viscosity, the slurries were prepared with 24 vol% of liquid MTES. Three different slurries were prepared and their compositions are detailed in Table 1. The notations M (Si–Al) and MP(Si–Al) correspond to slurries with only PMS and the PMS:PPS mixture in 2:1 volume ratio, respectively. The notations Si–Al and Si–3Al correspond to Si:Al filler volume ratios of 1:1 and 1:3 respectively. Firstly, the polymer precursor was dissolved in liquid MTES and subsequently the curing agents were added and homogenized by vigorous stirring for 10 min. Subsequent to this, Al and Si powders, which were previously mixed in a mortar and pestle, were added to the slurry, followed by further agitation for 15 min. Then the slurry was vacuum degassed (0.005 MPa for 3 min).

2.3. Tape casting

The slips were cast manually with an extensor on a silicone coated polyethylene terephthalate film. The gap between the extensor and the film was adjusted to 600 μm. The cast tapes were subsequently dried in air at room temperature for 48 h. After drying the green tapes were stripped from the film and cut into sheets 25 mm × 25 mm. The thickness of the green-tapes varied between 500 to 600 μm. Cross-linking was carried out by stepwise heating to 60 °C, 90 °C and then 120 °C with a dwell time of 4 h at each temperature.

2.4. Substrate pyrolysis and characterization

The green tapes were stacked and sealed in an alumina tube in N_2 atmosphere and pyrolyzed in an electric furnace. The substrates were pyrolyzed by giving four different treatments at final temperatures of 1000 °C/1 h, 1350 °C/2 h, 1400 °C/2 h

Table 1
Slurry compositions for tape casting process to obtain PDC substrates.

Compound	Slurry Composition (vol%)		
	M(Si–Al)	MP(Si–Al)	M(Si–3Al)
PMS-MK resin	45.0	30.0	45.0
PPS-H62 C	–	15.0	–
MTES	24.0	24.0	24.0
Si	15.0	15.0	7.5
Al	15.0	15.0	22.5
$Zr(acac)_3$	0.5	0.5	0.5
Oleic Acid	0.5	0.5	0.5

and 1500 °C/2 h. The heating and cooling rates were adjusted to 3 °C/min.

Differential thermogravimetric (TG) analysis of the non-pyrolyzed M(Si–Al) green substrate after cross-linking was carried out in a thermobalance (Perkin Elmer TGA-7) in nitrogen atmosphere by heating to 1000 °C and with a heating rate of 10 °C/min. The bulk densities of the pyrolyzed tapes were measured according to Archimedes's principle with distilled water as the immersion medium. Total open porosity, weight gain and total linear shrinkage after pyrolysis were determined. The coefficient of thermal expansion (CTE) was measured in tapes pyrolyzed at 1500 °C/2 h and compared with an Al_2O_3 substrate, using a heating rate of 5 °C/min up to 1000 °C in argon atmosphere (Netzsch- Dilatometer 402). The crystalline phases formed during pyrolysis at the different temperatures were determined by x-ray diffraction analysis (Rigaku Demax 2000) using Cu K_α radiation. The fracture surfaces of the substrates were examined by scanning electron microscopy (SEM- model Philips XL30). Transmission electron microscopy (TEM) was used to observe and identify the crystalline structures. The TEM observations were performed using a 200 kV TEM (JEM 200C) and a 300 kV HRTEM (JEM 3010 URP, 1.7 Point Resolution). The TEM specimens were prepared by cutting the as-pyrolyzed tapes into 3 mm diameter disks using an abrasion disk-cutter. The disks were mechanically ground to 150 μm. A further grinding step was performed using a dimple grinder, yielding a sample thickness of about 30 μm in the central region of the disk. Finally, the electron transparent regions in the specimens were achieved by argon ion beam thinning at beam energy of 6 kV. Specimens were coated with a thin layer of carbon to minimize electrostatic charging upon exposure to the electron beam.

3. Results and discussion

3.1. Pyrolysis and phase formation

TG and DTG curves of the non-pyrolyzed M(Si–Al) green substrate after cross-linking in N_2 atmosphere up to 1000 °C are shown in Fig. 1. The pyrolysis of the tape shows that most of the weight loss occurred in two steps, located around 200 and 750 °C. The initial weight loss step, which started at 150 °C is similar to that observed in as-received PMS-MK [21], indicating that the cross-linking process of the tape was incomplete. The first weight loss is attributable to cross-linking reactions within the siloxane resin, with release of gaseous by-products, or to evaporation of low molecular weight components occurring before such reactions link all the polymeric chains into a three dimensional network. The second weight loss can be attributed to transformation of the organic-inorganic polymeric network with cleavage of Si–(CH_3) bonds and volatilization of CH_4 [22]. A large weight gain is observed at temperatures between 780 and 900 °C. When active Al and Si are added to polysiloxane, a series of reactions may occur during pyrolysis with formation of various by-products like Al_4C_3 and Si [23,24]. This weight increase is related to Al powder or the by-product Al_4C_3 reacting with N_2 to form AlN. It is known that Al powders readily react with N_2 gas even at low temperatures, but the weight increase is slow because the diffusion of N_2 gas into metallic Al is hindered by the thin Al_2O_3 film on the Al powder surface [23]. The weight loss due to the degradation of the polymer is progressively compensated, between 200 and 800 °C by a small increase due to nitridation of the Al powder. During melting and above the melting temperature of Al (T_m=660 °C) the nitridation of Al is accelerated. On the other hand, silicon powder is not supposed to react either with polymer pyrolysis products or with nitrogen in this temperature range [7,24].

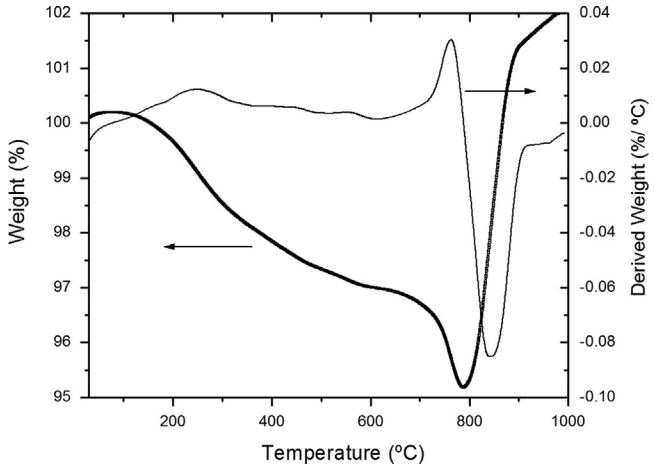

Fig. 1. TG and DTG curves of the non-pyrolyzed green M(Si–Al) substrate after cross-linking in N_2 atmosphere (heating rate:10 °C/min).

In Fig. 2 the XRD patterns of the substrates pyrolyzed in nitrogen at various temperatures are shown. The identified crystalline phases in substrates pyrolyzed at 1000 °C/1 h are Si, AlN and β-SiC (Fig. 2a). Aluminum peaks were not identified indicating reaction between aluminum or by-products containing Al with N_2 in the atmosphere to form AlN, and consequent reduction in the amount of metallic Al in the materials. What is surprising is that even at 1000 °C we can observe the formation of a large amount of β-SiC, since polysiloxane is known to yield only very poorly crystalline SiC up to 1600 °C. Moreover, Si powder added as filler is not expected to react with the decomposition products of the polymer even with the Si–O–C glass at this temperature [24]. One possible reason for the high amount of β-SiC formation is the development of metallic Si from the polymer precursor as an effect of Al over the Si–O–C matrix accelerating its ceramization process [10]. These findings lead to the conclusion that at pyrolysis temperatures below 1000 °C, Al readily reacts with free carbon and/or hydrocarbons which are parts of the Si(O,C) matrix as per reaction (1) below [11]:

$$SiOC + 6\ Al \rightarrow Al_2O_3 + Al_4C_3 + 3\ Si \quad (1)$$

Although crystalline Al_2O_3 was not identified on substrates pyrolyzed at 1000 °C, small peaks of α-Al_2O_3 could be identified at temperature above 1350 °C. The by-products such as Al_4C_3 and Si, react gradually with N_2 in the atmosphere to produce AlN and SiC. This reaction is carried out nearly to completion when pyrolysis temperature increases to 1000 °C [23]:

$$Al_4C_3 + 3\ Si + 2\ N_2 \rightarrow 4\ \ AlN + 3\ \ SiC \quad (2)$$

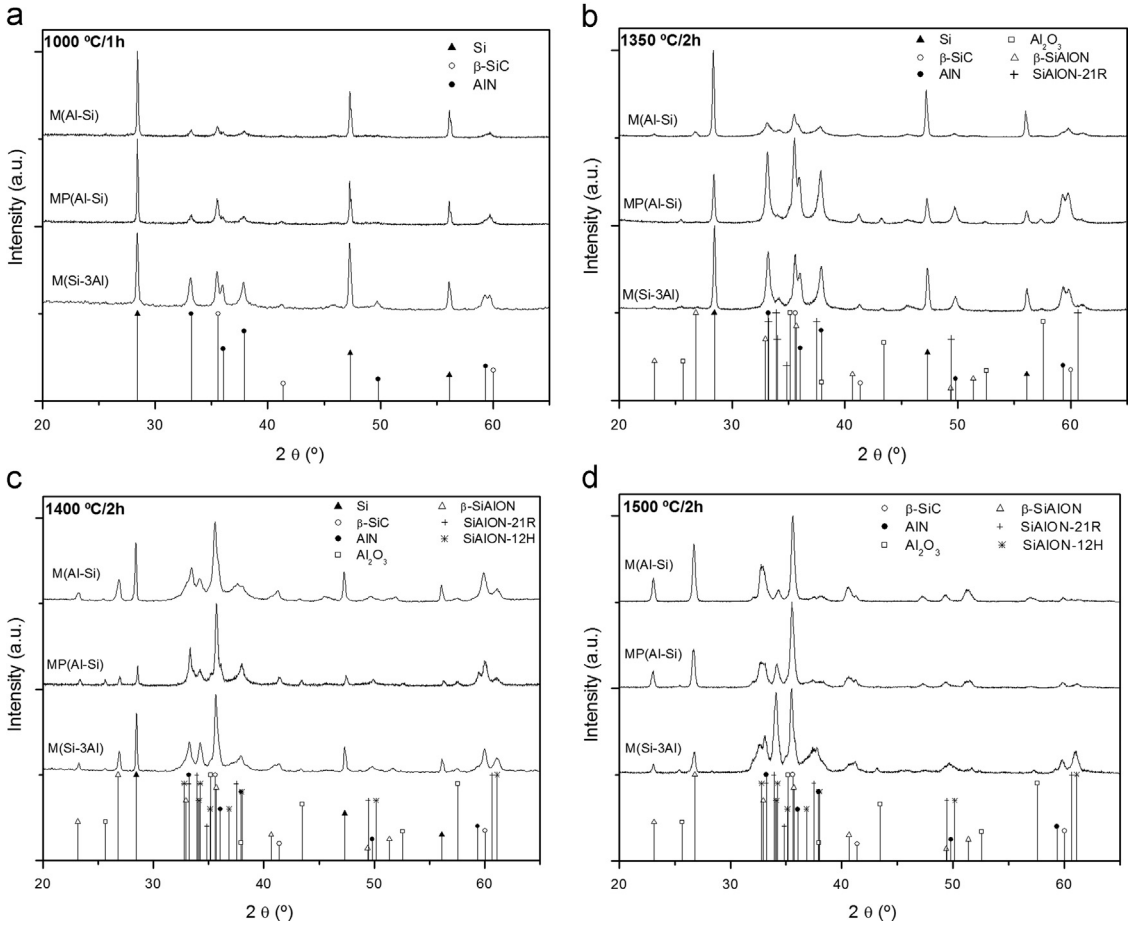

Fig. 2. XRD patterns of the PDC substrates after pyrolysis at different temperatures: (a) 1000 °C/1 h, (b) 1350 °C/2 h, (c) 1400 °C/2 h and (d) 1500 °C/2 h in N_2 atmosphere.

The ratio between Si and SiC decreases with increasing pyrolysis temperature in all compositions. As a relative measure, the peak intensity (peak height) of Si reflection at 28.4 ° was divided by the peak intensity of SiC reflection at 35.6 °, ($I_{28.4}/I_{35.6}$), and shown in Table 2. Sample MP(Si–Al), which contains a slightly higher amount of carbon, shows higher SiC formation than sample M(Si–Al), having the same amount of Si. On the other hand, sample M(Si–3Al) with the same polymeric phase but smaller amount of Si shows much higher SiC formation at temperatures up to 1350 °C. From these observations we can state that β-SiC formation is favored up to 1000 °C by the carbon content of the polymer and the aluminum concentration.

The peak intensities of AlN and β-SiC in samples treated at temperature of 1350 °C/2 h increase and some small peaks of β-SiAlON and SiAlON polytypoids as 21R ($SiAl_6O_2N_6$) and 12H ($SiAl_5O_2N_5$) were identified (Fig. 2b). As the heat treatment temperature increases (1400 °C/2h), the peaks of Si and AlN weaken, while those of β-SiAlON and SiAlON polytypoids become more evident (Fig. 2c). At this temperature Si is expected to react with the polymer derived matrix and form SiO gas which can react with AlN and the N_2 in the atmosphere to form phases in the SiAlON system. In the absence of Al, SiO would react with N_2 and form silicon oxynitride at temperature above 1200 °C [7]. As this crystalline phase was not found in any sample treated at the various temperatures, we can presume that β-SiAlON is preferentially formed instead of silicon oxynitride, according to reaction (3):

$$3\ SiO_{(g)} + 3\ AlN_{(s)} + N_{2(g)} \rightarrow Si_3Al_3O_3N_5 \quad (3)$$

Silicon reactivity increases as it reaches its melting temperature (1414 °C). Above this temperature, however, the silicon may react directly with the remaining Al_2O_3, as shown in reaction (4):

$$3\ Si_{(l)} + Al_2O_{3(s)} + AlN_{(s)} + 2N_{2(g)} \rightarrow Si_3Al_3O_3N_5 \quad (4)$$

Table 2
Ratio of intensities of Si and SiC XRD reflections for PDC substrates pyrolyzed at various temperatures.

Temperature (°C)	$I_{28.4}/I_{35.6}$		
	M(Si–Al)	MP(Si–Al)	M(Si–3Al)
1000	6.8	3.2	1.9
1350	3.7	0.6	1.5
1400	0.8	0.3	0.9

Increasing the pyrolysis temperature to 1500 °C/2 h resulted in a marked reduction in Si content and significant increase in β-SiAlON on substrates with Al:Si ratio of 1:1. Phases 21R, 12H and 15R SiAlON polytypoid were identified in all compositions, but they were predominant on substrate with higher amount of Al, M(Si–3Al) (Fig. 2d). These polytypoid phases can be formed by direct reaction of AlN and SiO_2 that originated from the decomposition of polymer matrix, see reaction (5):

$$6\ AlN_{(s)} + SiO_{2(s)} \rightarrow SiAl_6O_2N_6 \quad (5)$$

Microstructural examination of the samples by TEM showed very similar microstructure for samples pyrolyzed at 1500 °C regardless of their composition, and was composed mainly of elongated polytypoid grains, equi-axed grains and an amorphous phase. Fig. 3 shows a representative low magnification TEM bright field micrograph of elongated SiAlON polytypoid grains with the corresponding selected-area electron diffraction (SAED) which were observed in sample MP(Si–Al). The polytypoid phases generally form plate-like or needle-shaped grains which are expected to have a strengthening and toughening effect on the matrix phases by crack deflection, grain pull-out, or grain-bridging mechanisms.

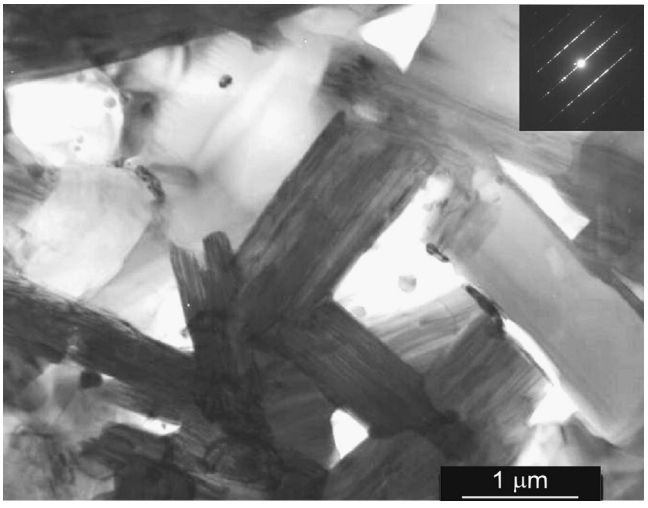

Fig. 3. TEM micrograph of typical elongated SiAlON polytypoid crystal with the corresponding SAED pattern.

The polytypoids 21R ($SiAl_6O_2N_6$), 12H ($SiAl_5O_2N_5$) and 15R ($SiAl_4O_2N_4$) were the major polytypoid phases observed as single-phase grains in substrates by HREM. In the Si–Al–O–N system, at the compositions between β-SiAlON and AlN, there are six polytypoid phases (8 H, 15R, 12H, 21R, 27R and 2 H), and these structures are labeled by Ramsdell notation, nR (rhombohedral) or nH (hexagonal) [25,26]. For the nR-type polytypoids, the unit cell consists of three rhombohedrally related sub-blocks which are separated by planar inversion domain boundaries (IDBs), and in each sub-block there are $(n/3-1)$ hexagonal layers. For the nH-type polytypoids, the unit cell consists of two hexagonal related sub-blocks separated by planar IDBs, and in each sub-block there are $(n/2-1)$ hexagonal layers [27]. Fig. 4 shows HREM images of a polytypoid grain and an enlarged image of a 12 H polytypoid grain. The alternating black–white contrast stripes related to the planar IDBs can be observed. Hexagonal 12 H SiAlON polytypoid with lattice parameters $a=0.30$ nm and $c=3.27$ nm could be fully identified. The larger numbers represent the number of layers inside each polytypoid sub-block, and the corresponding lattice distances are marked with smaller numbers. Fig. 5 shows images of the 21R SiAlON polytypoid. The lattice parameters of this phase are $a=0.30$ nm and $c=5.65$ nm. Most of the sub-blocks contain 6 layers and lattice distance of 1.88 nm. Fig. 6 shows image of a 15R polytypoid with most of the sub-blocks with 4 layers and a lattice distance of 1.40 nm. The lattice parameters of the 15R polytypoid have been determined to be $a=0.30$ nm and $c=4.18$ nm.

3.2. Polymer derived ceramic substrates

Ceramic substrates processed from polysilsesquioxane and Al and Si filler slurries exhibit homogeneous surface and good

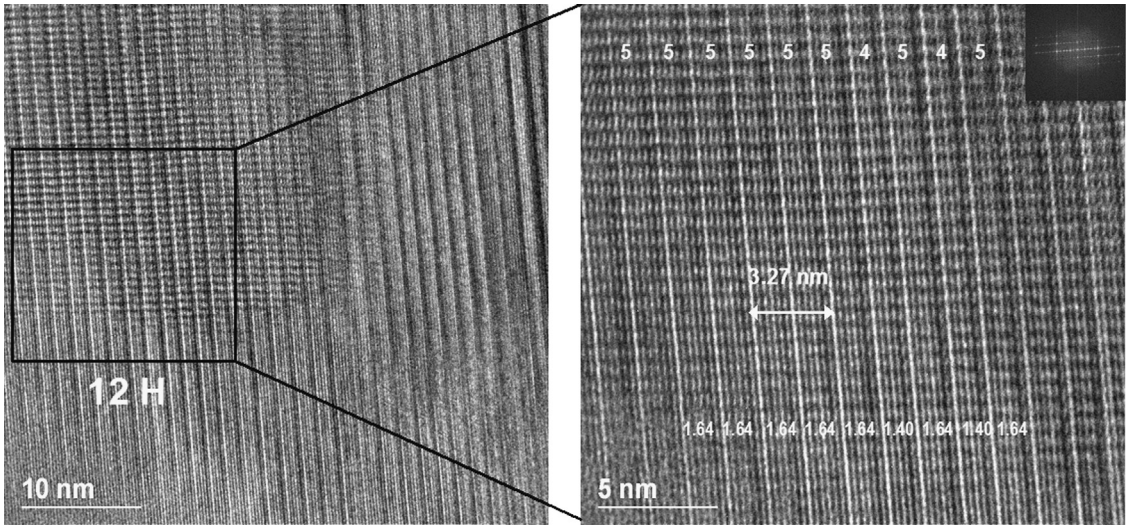

Fig. 4. HRTEM images of the 12 H SiAlON polytypoid grain.

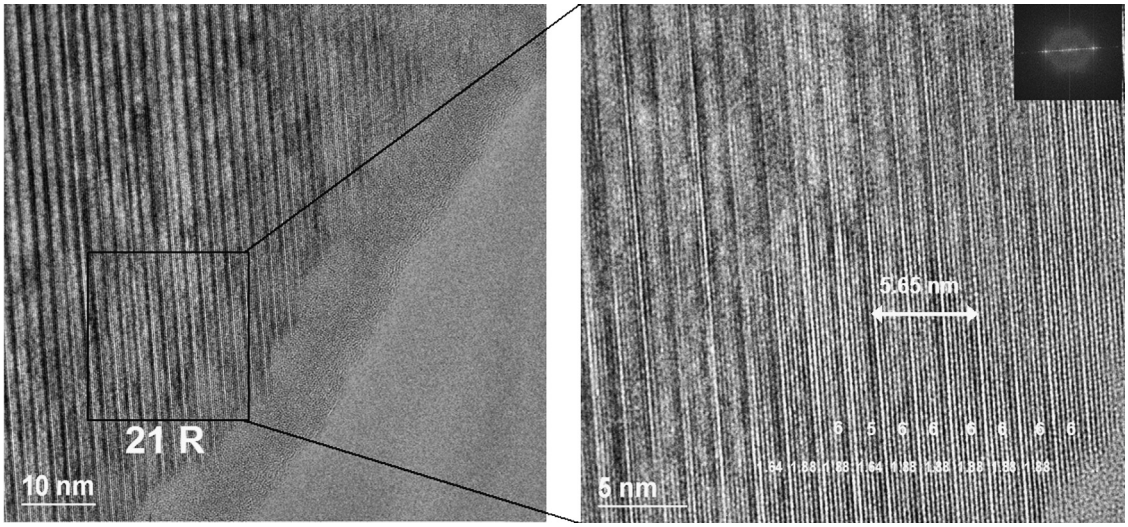

Fig. 5. HRTEM images of the 21R SiAlON polytypoid grain.

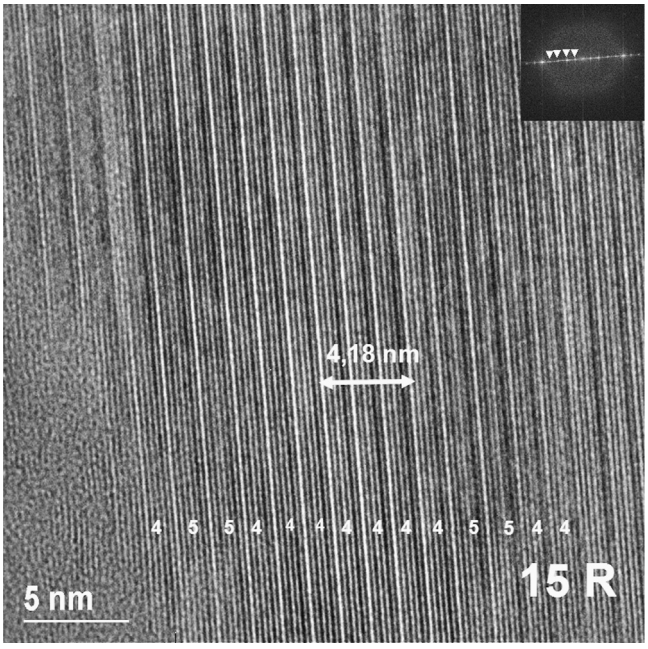

Fig. 6. HRTEM image of the 15R SiAlON polytypoid grain.

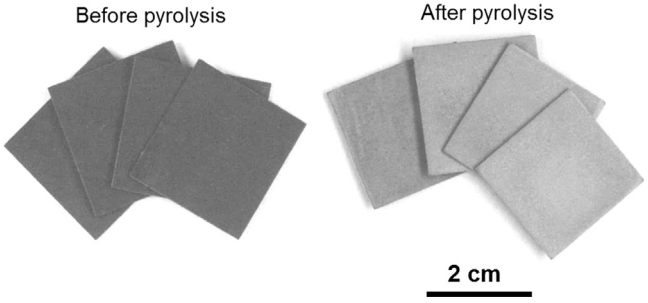

Fig. 7. PDC substrates before and after pyrolysis at 1500 °C/2 h.

Table 3
Characterization results of the substrates pyrolyzed at 1500 °C/2 h in N_2: Bulk density, total weight gain, open porosity, total linear shrinkage and coefficient of thermal expansion.

sample	Density (g/cm^3)	Weight gain (%)	Open porosity (%)	Linear shrinkage (%)	CTE ($\times 10^{-6}$ °C^{-1})
M(Si–Al)	2.27 ± 0.02	14.6 ± 0.5	25.4 ± 0.9	3.6 ± 0.2	5.34 ± 0.02
MP(Si–Al)	2.24 ± 0.02	15.5 ± 0.7	25.3 ± 0.07	3.9 ± 0.8	5.18 ± 0.02
M(Si–3Al)	2.34 ± 0.02	16.5 ± 0.7	24.3 ± 0.4	3.3 ± 0.6	6.50 ± 0.01

mechanical integrity without cracks and warps after pyrolysis at 1500 °C/2 h in N_2 (Fig. 7). Warping was avoided by a face-to-face lamination procedure.

Table 3 shows the characterization results of the substrates pyrolyzed at 1500 °C/2 h. To determine the total weight increase after pyrolysis, the substrates were weighed before and after pyrolysis. During pyrolysis, the weight loss due to polymer decomposition and formation of gaseous species by reactions with the filler is compensated by consumption of nitrogen by the Al filler to form AlN. The total weight gain of the sample M(Si–3Al) was slightly higher than that of M(Al–Si), because of the higher Al content in the former. Substrates showed low linear shrinkage, around 3.5%, which is a good result for near net shape applications. Considering the bulk density and the total open porosity, the skeleton density would approximate to 3.1 g/cm^3, which is close to final ceramic composition.

The porosity of the substrates can be observed in SEM images of the fracture surface (Fig. 8). The larger pores may have formed during the first stage of pyrolysis at low temperatures, below 300 °C, when some cross-linking gaseous products are released and produce some bubbles. Some whisker and platelet structures can be observed inside the

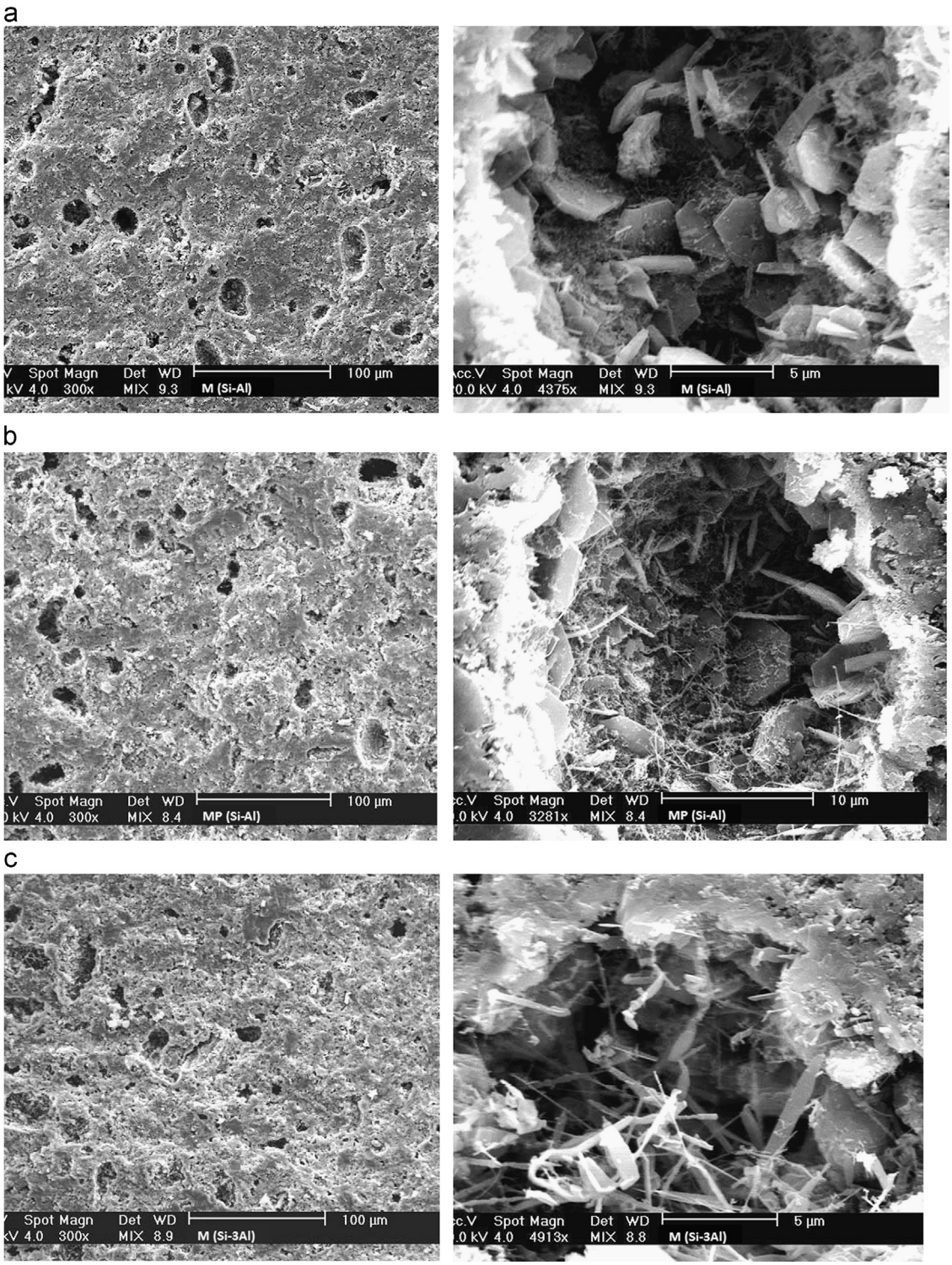

Fig. 8. SEM images of the fracture surface of the substrates pyrolyzed at 1500 °C/2 h in N_2, left side is a general view image and the right side shows details inside the pores: (a) M(Si–Al), (b) MP(Si–Al), (c) M(Si–3Al).

larger pores. Normally such structures are formed involving gaseous species, and as expected, the reaction with SiO gas to form SiAlON phases.

The coefficient of thermal expansion of the substrates were measured and compared with an alumina substrate (Fig. 9). Substrates with the same Al and Si concentration, but with different initial polymer composition showed practically the same CTE (Table 3). On the other hand substrate with higher amounts of Al showed a slightly higher CTE as a result of formation of different crystalline phases during pyrolysis. These results show how the CTE can be tailored by the starting filler composition.

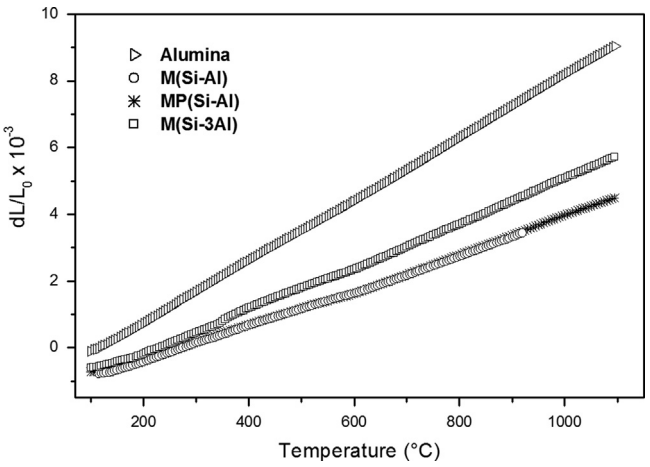

Fig.9. Curves of thermal expansion up to 1000 °C of the PDC substrates pyrolyzed at 1500 °C/2 h and Al_2O_3 substrate.

4. Conclusions

Si and Al loaded silane/polysilsesquioxane slurries were used to prepare ceramic substrates in the Si–Al–O–N–C system using the tape-casting process. PDC substrates of β-SiC/SiAlON composites were successfully obtained after pyrolysis at temperature of 1500 °C/2 h in N_2 atmosphere. Pyrolysis at intermediate temperatures allowed understanding of phase formation, depending on substrate composition. A substrate with a higher amount of carbon showed formation of more β-SiC. β-SiAlON predominates in samples with higher Si content while SiAlON polytypoids were more significant in the sample with higher Al concentration. The 21R ($SiAl_6O_2N_6$), 12H ($SiAl_5O_2N_5$) and 15R ($SiAl_4O_2N_4$) SiAlON polytypoids were observed and identified by HREM. The characteristics of these materials seem promising for their application not only as PDC substrates but also as thick coatings, which can resist severe environment, application in ceramic joining and low-cost matrix source in ceramic matrix composites.

Acknowledgments

The authors acknowledge the Brazilian Nanotechnology National Laboratory for training and allowing operation of the HTREM under proposal TEM 5015.

References

[1] P. Colombo, G.M.R. Riedel, G.D. Soraru, Polymer-derived ceramics: 40 years of research and Innovation in advanced ceramics, J. Am. Ceram. Soc. 93 (2010) 1805–1837.
[2] P. Greil, Active-filler-controlled pyrolysis of preceramic polymers, J. Am. Ceram. Soc. 78 (1995) 835–848.
[3] P. Greil, Near net shape manufacturing of polymer derived ceramics, J. Eur Ceram. Soc. 76 (1998) 1905–1914.
[4] P. Cromme, M. Scheffler, P. Greil, Ceramic tapes from preceramic polymers, Adv. Eng. Mater. 4 (2002) 873–877.
[5] R.M. Rocha, M. Scheffler, P. Greil, J.C. Bressiani, A.H. A. Bressiani, ceramic tapes of Si–Al–O–N–C compounds using mixtures of polyssiloxane and Si–Al_2O_3 fillers, Ceramica 51 (2005) 42–51.
[6] C.R. Rambo, H. Sieber, Manufacturing of cellular β-SiAlON/β-SiC composite ceramics from cardboard, J. Mater. Sci. 41 (2006) 3315–3322.
[7] M. Scheffler, E. Pippel, J. Woltersdorf, P. Greil, In situ formation of SiC–Si_2ON_2 micro-composite materials from preceramic polymers, Mat. Chem. Phys. 80 (2003) 565–772.
[8] R.M. Rocha, C.A.A. Cairo, M.L.A. Graça, Formation of carbon fiber-reinforced ceramic matrix composites with polysiloxane/silicon derived matrix, Mater. Sci. Eng. A 437 (2006) 268–273.
[9] J. Anggono, Brian Derby, Pyrolysis of aluminium loaded polymethylsiloxanes: the influence of Al/PMS ratio on mullite formation, J. Mater. Sci. 45 (2010) 233–241.
[10] M. Narisawa, H. Kado, H. Mabuchi, Y.W. Kim, Accelerated ceramization of polymehylsilsesquioxane by aluminum-based filler reductant, Appl. Organometal. Chem. 24 (2010) 612–617.
[11] L Toma, C. Fasel, S. Lauterbach, H.J. Kleebe, R. Riedel, Influence of nano-aluminum filler on the microstructure of SiOC ceramics, J. Eur. Ceram. Soc. 31 (2011) 1779–1789.
[12] K.H. Jack, Sialons and related nitrogen ceramics-review, J. Mater. Sci. 11 (1976) 1135–1158.
[13] J.G. Lee, I. Cutler, Sinterable sialon powder by reaction of clay with carbon and nitrogen, Am. Ceram. Bull. 598 (1979) 869–871.
[14] J.Y. Qiu, J. Tatami, C. Zhang, K. Komeya, T. Meguro, Y.B. Cheng, Influence of starting material composition and carbon content on the preparation of Mg-α sialon powders by carbothermal reduction–nitridation, J. Eur. Ceram. Soc. 22 (2002) 2989–2996.
[15] A.D. Mazzoni, E.F. Aglietti, Mechanism of the carbonitriding reactions of SiO_2–Al_2O_3 minerals in the Si–Al–O–N system, Appl. Clay Sci. 12 (1998) 447–461.
[16] J.J. Li, J. Wang, H.Y. Chen, B.D. Sun, J.B. Jia, Synthesis of β-sialon–AlN polytypoid ceramics from aluminum dross, Mater. Trans. 51 (2010) 844–848.
[17] E. Bernardo, G. Parcianello, P. Colombo, J.H. Adair, A.T. Barnes, J.R. Hellmann, B.H. Jones, J. Kruise, J.J. Swab, SiAlON ceramics from preceramic polymers and nano-sized fillers: application in ceramic joining, J. Eur. Ceram. Soc. 32 (2012) 1329–1335.
[18] E. Bernardo, P. Colombo, S. Hampshire, SiAlON-based ceramics from filled preceramic polymers, J. Am. Ceram. Soc. 89 (2006) 3839–3842.
[19] R. Harshe, C. Balan, R. Riedel, Amorphous Si(Al)OC ceramic from polysiloxanes: bulk ceramic processing, crystallization behavior and applications, J. Eur. Ceram. Soc. 24 (2004) 3471–3482.
[20] J. Cordelair, P. Greil, Electrical conductivity measurements as a microprobe for structure transitions in polysiloxane derived Si–O–C ceramics, J. Eur. Ceram. Soc. 20 (2000) 1947–1957.
[21] T. Takahashi, P. Colombo, SiOC ceramic foams through melt foaming of a methylsilicone preceramic polymer, J. Porous Mater. 10 (2003) 113–121.
[22] G.M. Relund, S. Prochazka, R.H. Doremus, Silicon oxycarbide glasses: Part I. Preparation and chemistry, J. Mater. Res. 6 (1991) 2716–2722.
[23] Z. Xie, S. Wang, Z. Chen, Active filler (aluminum-aluminum nitride) controlled polycarbosilane pyrolysis, J. Inorg.Org. Polym. Mater. 16 (2006) 69–81.
[24] Q. Wei, E. Pippel, J. Woltersdorf, M. Scheffler, P. Greil, Interfacial SiC formation in polysiloxane-derived Si–O–C ceramics, Mater. Chem. Phys. 73 (2002) 281–289.
[25] J. Grims, S. Esmaeilzadeh, G. Svensson, Z.J. Shen, High-resolution electron microscopy of a Sr-containing Sialon polytypoid phase, J. Eur. Ceram. Soc. 19 (1999) 2723–2730.
[26] C.S. Lee, X.F. Zhang, G. Thomas, Novel joining of dissimilar ceramics in the Si_3N_4–Al_2O_3 system using polytypoids functional gradients, Acta Mater. 49 (2001) 3775–3780.
[27] Y. Yu, I.L. Tangen, T. Grande, R. Hoier, M.A. Einarsrud, HRTEM investigations of new polytypoids in the high-AlN region of the AlN–Al_2O_3–Y_2O_3 system, J. Am. Ceram. Soc. 87 (2004) 275–278.